Analysis of large experimental datasets in electrochemical impedance spectroscopy

Article *in* Analytica chimica acta · September 2012

DOI: 10.1016/j.aca.2012.06.055 · Source: PubMed

1 author:

Aliaksandr S Bandarenka
Technische Universität München
90 PUBLICATIONS **2,877** CITATIONS

SEE PROFILE

Analytica Chimica Acta 743 (2012) 41–50

Contents lists available at SciVerse ScienceDirect

Analytica Chimica Acta

journal homepage: www.elsevier.com/locate/aca

Analysis of large experimental datasets in electrochemical impedance spectroscopy

Alexander S. Bondarenko*

Center for Electrochemical Sciences – CES, Ruhr-Universität Bochum, Universitätstr. 150, D-44780 Bochum, Germany

HIGHLIGHTS

- An approach to the analysis of multidimensional impedance data has been developed.
- The approach uses successive Bayesian estimation and a new hybrid optimisation algorithm.
- The performance of the approach has been evaluated using simulated and experimental data.

GRAPHICAL ABSTRACT

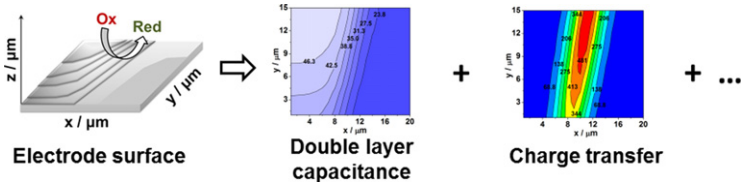

ARTICLE INFO

Article history:
Received 25 May 2012
Received in revised form 21 June 2012
Accepted 29 June 2012
Available online 14 July 2012

Keywords:
Electrochemical impedance spectroscopy
Multidimensional data analysis
Successive Bayesian estimation
Complex nonlinear least squares method
Hybrid algorithms

ABSTRACT

An approach for the analysis of large experimental datasets in electrochemical impedance spectroscopy (EIS) has been developed. The approach uses the idea of successive Bayesian estimation and splits the multidimensional EIS datasets into parts with reduced dimensionality. Afterwards, estimation of the parameters of the EIS-models is performed successively, from one part to another, using complex nonlinear least squares (CNLS) method. The results obtained on the previous step are used as *a priori* values (in the Bayesian form) for the analysis of the next part. To provide high stability of the sequential CNLS minimisation procedure, a new hybrid algorithm has been developed. This algorithm fits the datasets of reduced dimensionality to the selected EIS models, provides high stability of the fitting and allows semi-automatic data analysis on a reasonable timescale. The hybrid algorithm consists of two stages in which different zero-order optimisation strategies are used, reducing both the computational time and the probability to overlook the global optimum. The performance of the developed approach has been evaluated using (i) simulated large EIS dataset which represents a possible output of a scanning electrochemical impedance microscopy experiments, and (ii) experimental dataset, where EIS spectra were acquired as a function of the electrode potential and time. The developed data analysis strategy showed promise and can be further extended to other electroanalytical EIS applications which require multidimensional data analysis.

1. Introduction

Impedance spectroscopy is one of the most powerful non-destructive methods of investigating the boundaries between materials with different types of conductivities. Electrochemical impedance spectroscopy (EIS) [1] is mostly used to probe the interfaces between electronically conducting solid electrodes and ionically conducting electrolytes, where both electrode and electrolyte can be either liquid or solid [2].

EIS is based on the analysis of interactions between an object and alternating current (*ac*) probing signals of different frequencies. The *ac* response of electrochemical systems is highly frequency dependent and contains valuable information about different processes which take place simultaneously at the electrode|electrolyte interface [3]. EIS data analysis allows reconstruction of the properties of systems under investigation and estimation of their key physico-chemical parameters.

* Correspondence address: Universitätsstr. 150, NC 4/73, D-44780 Bochum, Germany. Tel.: +49 0234 32 29433.
E-mail address: aliaksandr.bandarenka@rub.de

0003-2670/$ – see front matter © 2012 Elsevier B.V. All rights reserved.
http://dx.doi.org/10.1016/j.aca.2012.06.055

Classical EIS data analysis consists of two stages: (i) elucidation of an appropriate physical model of the system and (ii) fitting of EIS data to the model to estimate the parameters of the models. More than one hundred years of history of EIS enriched this method with efficient theoretical tools for powerful elucidation of physical models of many different electrochemical systems. However, one of the main impediments to a wider and more efficient application of EIS-based approaches in different areas (not only in electroanalytical chemistry, but also physics, biology and medicine) is the ability to process large data sets of impedance data on a reasonable timescale, i.e. fulfilling step (ii) for large datasets and short timeframes. While recent efforts in the field of multidimensional EIS datasets processing are focused on extraction of analytical information for sensor and bio-sensor applications [4–6], estimation of parameters of physical models remains difficult in case of large EIS datasets.

Modern equipment can currently acquire large amount of impedance spectra fast enough to collect EIS data, as a function of time or electrode potentials, at rates suitable to investigate markedly non-stationary electrochemical processes [7–10] or even to perform real-time monitoring of human tissue properties *in vivo* [11]. Nevertheless, EIS spectra analysis remains a largely time consuming process in which each single spectrum is processed individually. The origin of this situation can be attributed to the intrinsic properties of electrochemical systems which are highly nonlinear systems.

The parameters of electrochemical systems can change drastically even if the experimental conditions are only slightly altered. For example, the currents caused by electrochemical reactions, i_{Faradaic}, are exponential functions of the electrode potential, E, and, at the same time, complex non-linear functions of the surface concentrations, C_s, of reagents and products. The surface concentrations are determined by the properties of the electrode|electrolyte interface which are, in turn, extremely difficult or impossible to predict analytically, even with the help of modern theoretical concepts.

Due to these complexities, analysis of multidimensional EIS data is not a trivial task. The successful optimisation of an individual impedance spectrum does not guarantee a successful routine fitting of an entire multidimensional impedance dataset. Algorithms which are used in modern EIS are, unfortunately, not stable enough and often fail to provide automatic or semi-automatic fitting modes.

In this work, an approach for the analysis of large experimental datasets in EIS has been developed. It uses successive Bayesian estimation [12–14] and splits the EIS-datasets into parts with reduced dimensionality. Afterwards, estimation of the parameters of the EIS-models is performed successively, using complex nonlinear least squares (CNLS) method. The results obtained on the previous step are then used as *a priori* values for the analysis of the next part. To provide stability of the CNLS-minimisation procedures, a new hybrid algorithm has been also developed. This algorithm fits the datasets of reduced dimensionality to the selected EIS-models and provides required stability of the fitting to allow semi-automatic data analysis on a reasonable timescale. The performance of the developed data analysis approach has been evaluated by using simulated and experimental EIS datasets.

2. Problem formulation

A typical impedance spectrum measured in classical electrochemical impedance spectroscopy is shown in Fig. 1A. This spectrum is the dependence of the real part of impedance ($\text{Re}[Z] = |Z| \cos\varphi$) and the imaginary part ($\text{Im}[Z] = |Z| \sin\varphi$) on the frequency, f, of the *ac* probing signal, where $|Z|$ is the absolute value

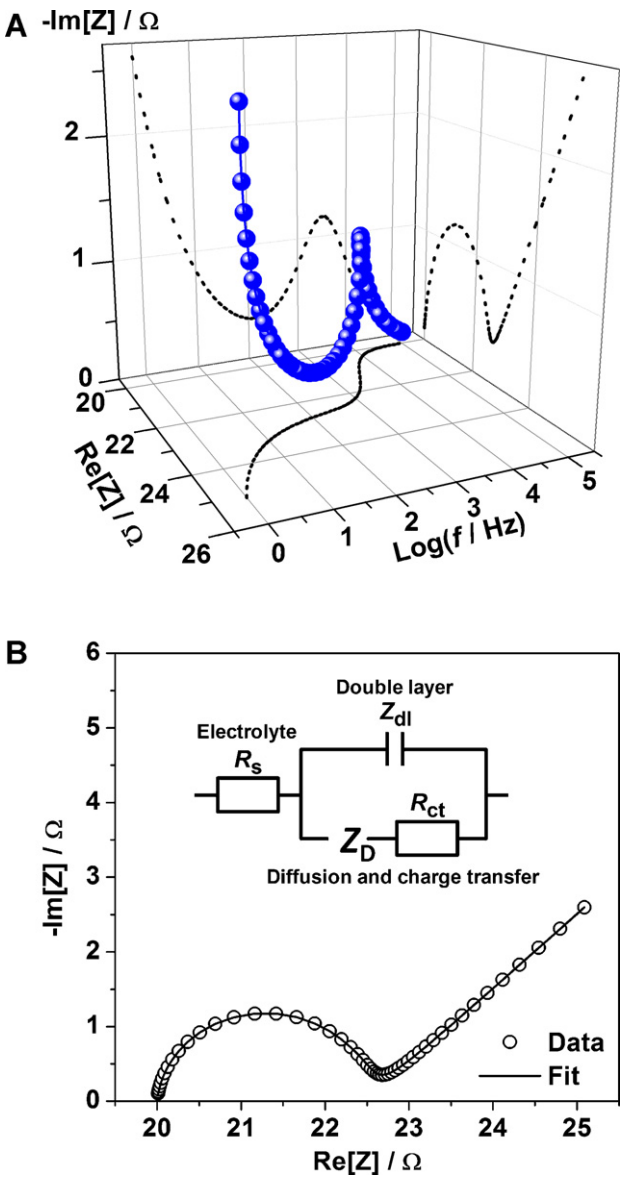

Fig. 1. (A) A three-dimensional representation of a single impedance spectrum (simulated) which is a dependence of the real and imaginary parts of the impedance on frequency of the *ac* probing signal (f). (B) The same spectrum as (A) but presented as a function of the real part of impedance on the imaginary part. Inset to (B) shows a typical physical model of an electrochemical interface in terms of equivalent electric circuits (R_{ct} – charge transfer resistance, Z_D – the mass transfer impedance, Z_{dl} – impedance of the electric double layer, R_s – the electrolyte resistance, see text for further details). Solid line in (B) shows the fitting of the data to the model.

of impedance (the ratio between the amplitudes of the probing signal and current response) and φ is the measured phase shift between the probing signal and the response. Therefore, the classical impedance spectrum is a following dataset:

$Re[Z]$; $Im[Z]$; probing *ac* frequency

The alternative representation of the experimental EIS datasets uses the measured absolute values of impedance and the phase shift:

$|Z|$; φ; probing *ac* frequency

Fig. 1B shows a 2D representation of the same spectrum, on the Re[Z]/−Im[Z] plane. Once the physical model of the system has been elucidated, the CNLS fitting procedures can be applied to calculate the parameters of the model from the EIS spectra.

In classical EIS, physical models of the electrochemical interface are expresssed in terms of either equations or so-called equivalent electric circuits (EECs). For example, the EEC shown in Fig. 1B, is equivalent to the following equation describing the EIS response in case of an electrochemical reaction with diffusion limitations:

$$Z(j\omega) = R_s + \left((j\omega)^n C'_{DL} + \frac{1}{R_{ct} + Z_T(j\omega)}\right)^{-1} \quad (1)$$

where $\omega = 2\pi f$ is the angular frequency; C'_{DL} and the CPE[1]-exponent n describe the response of the double layer; $R_{ct} = -1/(\partial i_{Faradaic}/\partial E)$ is the charge transfer resistance; Z_T is a mass transport impedance, which is usually represented by the Warburg impedance, $Z_W = A_W(j\omega)^{-0.5}$; A_W is the Warburg coefficient, R_s is the electrolyte resistance and j is the imaginary unit. The physical model which is defined by Eq. (1) is one of the most frequently used EIS-models: it describes correctly the response of many common electrochemical systems. This non-linear model has 5 parameters to estimate: R_s, R_{ct}, C'_{DL}, n, A_W. While there are many other models which describe different electrochemical systems, the model defined by Eq. (1) will be used further in this work as the most typical one.

In order to find the parameters P_k of impedance models based on experimental impedance spectra, the CNLS method was developed few decades ago [15–17]. In this approach, the following sum of residuals r^2 is minimised:

$$r^2 = \frac{1}{m-k}\sum_{i=1}^{m}\left\{w'_i\left[ReZ_i(f_i) - ReZ_{i,calc}(f_i, P_k)\right] + w''_i\left[ImZ_i(f_i) - ImZ_{i,calc}(f_i, P_k)\right]\right\}^2 \quad (2)$$

where m is the number of frequencies; k is the number of parameters; $\mathrm{Re}\,Z_i(f_i)$ and $\mathrm{Im}\,Z_i(f_i)$ are the real and imaginary parts of the impedance measured at a certain frequency f_i; $\mathrm{Re}\,Z_{i,calc}(f_i, P_k)$ and $\mathrm{Im}\,Z_{i,calc}(f_i, P_k)$ are the respective impedance values calculated using an appropriate model; w'_i and w''_i are appropriate statistical weights.

Currently, no minimisation algorithm can guarantee a straightforward identification of the global minima of complex objective functions such as function (2). Iterative minimisation procedures often fail to find a global minimum. The main difficulty is that the objective functions in EIS are non-linear and assigned implicitly and arbitrarily by the user in terms of equivalent electric circuits. Objective functions can, therefore, have very different topologies depending on the system properties.

Commercially available software [18–22] developed to process individual impedance spectra use a few well-known algorithms such as Levenberg–Marquardt algorithm [23,24], the Nelder–Mead down-hill simplex method [25] or genetic algorithms [26].

Nowadays, modern equipment allows acquisition of multidimensional EIS data such as impedance spectra recorded as a function of either time or electrode potential:

$Re[Z]$; $Im[Z]$; probing *ac* frequency; time; (3)

$Re[Z]$; $Im[Z]$; probing *ac* frequency; electrode potential; (4)

and larger datasets, which describe the impedance response as a function of frequency, time and the potential or as a function of frequency and spatial coordinates:

$Re[Z]$; $Im[Z]$; probing *ac* frequency; time; electrode potential; (5)

$Re[Z]$; $Im[Z]$; probing *ac* frequency; x-coordinate; y-coordinate; (6)

[1] CPE denotes the *c*onstant *p*hase *e*lement, a semi-empirical element which is widely used in EIS to describe the response of the electric double layer.

The latter dataset (6) represents a possible output of scanning electrochemical impedance microscopy experiments, as will be discussed later.

The analysis of the above-mentioned datasets is much more complicated compared to the inverse problem solution in classical EIS, i.e. in the case of individual spectra. However, it might be possible to solve it efficiently if the idea of the successive Bayesian estimation [12–14] would be combined with an efficient minimisation algorithm.

In many cases, the EIS-model remains formally the same, i.e. it can describe the whole EIS dataset. If the model defined by Eq. (1) is applicable, then the following set of estimated parameters is expected to be the output of the analysis procedure:

$$R_s(t);\ R_{ct}(t);\ C'_{DL};\ n(t);\ A_W(t); \quad (7)$$

and

$$R_s(E);\ R_{ct}(E);\ C'_{DL}(E);\ n(E);\ A_W(E); \quad (8)$$

for the datasets (3) and (4), correspondingly.

The set of parameters (7) describes the dependences of the parameters of the model (1) on time, while the set of parameters (8) shows how the parameters change with the electrode potential.

Similarly, for the datasets (5) and (6), the following set of parameters should be obtained:

$$R_s(t,E);\ R_{ct}(t,E);\ C'_{DL}(t,E);\ n(t,E);\ A_W(t,E); \quad (9)$$

and, respectively:

$$R_s(x,y);\ R_{ct}(x,y);\ C'_{DL}(x,y);\ n(x,y);\ A_W(x,y); \quad (10)$$

The set of parameters (9) is the surface showing how the parameters of the models change with both time and the electrode potential, while the set (10) describe the dependence of the parameters on spatial coordinates x and y.

The problem can be, therefore, formulated as follows: one should analyse the datasets (3)–(6) and estimate the corresponding parameter sets (7)–(10).

3. Method. Analysis of large datasets in EIS

As it was mentioned in Section 1, the main concept of this work is to use the idea of successive Bayesian estimation to split the multidimensional datasets into parts with reduced dimensionality. Estimation of the parameters of the models can be afterwards performed successively, from one part to another using complex nonlinear least squares (CNLS) method. However, it should be noted that other alternative strategies can be explored as well, such as artificial neural network analysis to replace successive Bayesian estimation, and differential impedance analysis [27] to replace CNLS.

This section briefly describes the application of the successive Bayesian estimation procedure for the analysis of the large EIS datasets and additionally describes a new hybrid optimisation algorithm which provides high stability of the CNLS-minimisation procedures. This algorithm fits the datasets of reduced dimensionality to the selected EIS-models and allows semi-automatic data analysis on a reasonable timescale.

3.1. Successive Bayesian estimation

One of the straightforward ways of how to split the large datasets is to consider them as a collection of normal "3D" spectra, such as the one shown in Fig. 1A. If the physical model of the electrochemical system is elucidated, the following formal procedure of data analysis can be implemented:

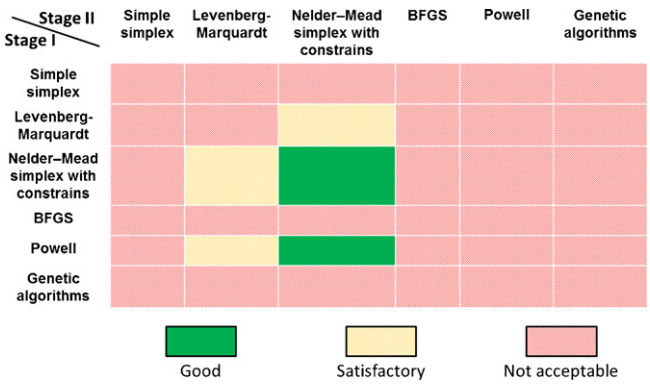

Fig. 2. Output of the algorithm screening procedure. Promising combinations of the common minimisation strategies were identified using large experimental EIS data-sets. These identified basic combinations were used to construct and improve the hybrid algorithm.

(1) Splitting of the large dataset to obtain a collection of "3D" spectra.
(2) Manual analysis and fitting of the 1st spectrum with reduced dimensionality using a CNLS method (minimisation of function (2)).
(3) Successive estimation of the parameters of the EIS-models, from one "3D" spectrum to another; the results obtained on the previous step are to be used as *a priori* values for the analysis of the next part.

Implementation of steps 1 and 2 can be done with relative ease. However, step 3 requires a stable minimisation algorithm in order to perform the analysis in automatic mode. As it was mentioned above, target function (2) has a complex topology and the position of the global minimum can change drastically even if e.g. electrode potential is changed just slightly. Unfortunately, well-established minimisation algorithms used in EIS could not provide the required stability to perform the analysis at step 3 in an automatic mode, even if the results obtained on the previous step were used as *a priori* values for the analysis of the next part. To provide the required stability, a new hybrid minimisation algorithm has been developed, as described in the following sections.

3.2. Hybrid algorithm development. Screening procedure

A minimisation algorithm which uses the Nelder–Mead downhill simplex with varying constraints has shown promise in processing datasets in potentiodynamic electrochemical impedance spectroscopy (Re[Z], Im[Z], frequency, electrode potential) [28–34]. However, it is not stable enough and less suitable to fit larger datasets (e.g. in case of a EIS-based microscopy: Re[Z], Im[Z], frequency, x, y), even with simulated data. Other well-known algorithms were also tested on large datasets but did not show the required stability. Therefore, the aim is to develop a (two)-stage hybrid algorithm providing stable sequential fitting or EIS data with reduced dimensionality.

To construct an efficient two-stage hybrid algorithm, a screening procedure was performed. At Stage I of the hybrid algorithm, it is important to have an optimisation strategy capable of efficiently identifying the general area of the global minimum based on *a priori* values obtained at the previous stage (Section 3.1). This strategy must always provide parameter values which are reasonably close to the global minimum irrespective of function topology, influence of random noise and any other relevant factors. At Stage II, the algorithm should be able to identify the exact position of the minimum.

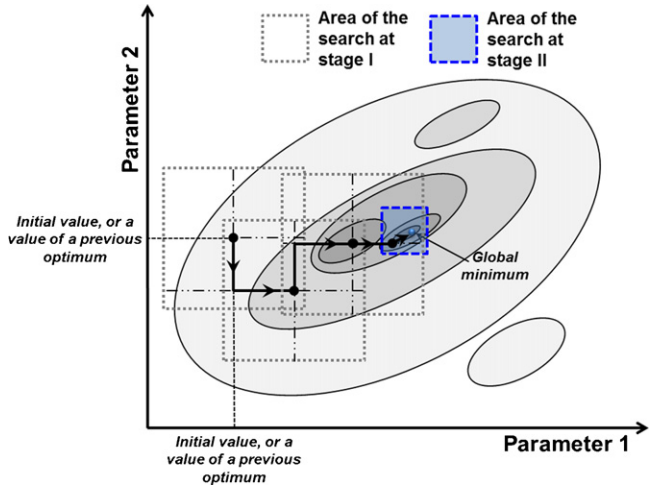

Fig. 3. A schematic representation of the optimisation procedure for the developed hybrid algorithm. A case with 2 optimisation parameters is presented. Grey areas schematically reflect the target function topology.

Fig. 2 shows the output of the screening procedure, where 6 common and widely used algorithms were tested in different combinations (36 combinations in total). To find the optimal combinations, different types of algorithms and their combinations were selected. These are: (i) optimisation (Simplex [35]), iterative (Levenberg–Marquardt [23]), and (ii) heuristic (Nelder–Mead [25]) methods and (1) the non-gradient (Nelder–Mead [25], Simplex, Genetic [26]) and (2) gradient (Levenberg–Marquardt [23], BFGS [36–39]) methods.

The evaluation criteria of the algorithm combinations were: (i) the computational time, (ii) accurate identification of the global minima of the functions of different topologies, and (iii) stability for the fitting of large experimental EIS data-sets. If (i) the total computational time was $\leq$20 s per spectrum (3 GHz processor, 4GB RAM), (ii) the algorithm combination was able to work accurately with functions of different topologies (practically, different EECs were used) and (iii) it fails in finding optima less than one time per 20 spectra in the automatic fitting mode using initial values from the previously identified minima, then the algorithm combination was evaluated as "good" (Fig. 2). If the algorithm combination does not pass the criterion (ii), it was evaluated as "satisfactory" (Fig. 2). Other cases were evaluated as "not acceptable" (Fig. 2).

As can be seen from Fig. 2, two promising combinations were found. These two algorithm combinations were tested further using simulated impedance data-sets to construct and optimise the hybrid algorithm. At this stage, the combination of the Powell algorithm and Nelder–Mead simplex (with constraints) minimisation strategies had shown the best performance of the tested combinations. However, a straightforward combination of these algorithms appeared not to be enough to achieve the required stability and performance of fitting for both experimental and simulated EIS data. Therefore, further optimisations were necessary.

3.3. Optimisation of the hybrid algorithm

The Powell algorithm (selected for the first optimisation stage of the hybrid algorithm) uses one-dimensional parameter optimisation at each iteration stage. However, once the EIS data analysis was performed, it was found that modifications to this strategy should be introduced so that the output of Stage (I) is close to the global minimum with the highest probability possible.

The modified strategy is schematically explained in Fig. 3. Stage (I) starts with an initial value which is either a position of the optimum calculated using a previously optimised spectrum from the

same dataset (see Section 3.1), or can be initially set by the user. One-dimensional optimisations are then performed within a range which primarily covers ±10% from the optimum in the parameter space (Fig. 3). The algorithm explores the whole of this parameter space to increase the probability of escape from a local minimum. If the minimum value is found at the border of the search area, the area expands by 30% compared to the previous iteration and the search is repeated. Otherwise, the optimised vector of the parameters moves towards the global minimum iteration-by-iteration, as shown schematically in Fig. 3. Most of the so-called zero-order optimisation algorithms were found to give reasonably good results at this stage to perform one-dimensional optimisation.

However, the obvious disadvantage of the strategy used at the first stage is that it experiences difficulties at the final stage to refine the position of the minimum. Nevertheless, a Nelder–Mead simplex (with constraints) algorithm can refine the exact position of the minimum very efficiently in Stage (II). The optimised value for the search area at Stage (II) was found to be around ±3% from the optimum found at the Stage (I), as schematically shown in Fig. 3.

It is important to emphasize that the stability of the hybrid algorithm can be controlled by several parameters. The most important parameter is the number of iterations involved in the first stage. The other parameters deal with the area of the search at both stages. The actual parameter values will depend on the datasets. However, a maximum of 300–700 iterations performed at the first stage of the hybrid algorithm gave a reasonably good stability of fitting for all the datasets used in this work. With a suitable algorithm now determined, evaluation of the overall strategy and the algorithm with model and experimental data was essential to ensure the quality of the method.

4. Evaluation of the developed method and examples

4.1. Simulated EIS dataset

Two different "5D" EIS datasets (simulated and experimental) were used to evaluate the developed method and the performance of the hybrid algorithm.

The following data-set was simulated using the classical model (equivalent electric circuit) shown in Fig. 1B with EIS Spectrum Analyser software [28]:

Re[*Z*]; *Im*[*Z*]; probing ac frequency; x – coordinate;

y – coordinate.

This simulated dataset is the same as (6) and can be considered as a collection of 300 individual impedance spectra[2] acquired locally at the surface of a hypothetical working electrode during scans along x and y directions. 50 different *ac* frequencies were used to simulate the EIS data. This dataset represents a possible output of localised impedance spectroscopy measurements [40,41] which might aim to map variations of the double layer capacitance, charge transfer resistance or other key parameters across an electrode surface.

Fig. 4A schematically shows the hypothetical electrode surface at which an electrochemical reaction takes place.

Fig. 4B–G shows the simulated dependences of the parameters of the impedance (modulus $|Z|$ and the phase shift φ)[3] on spatial coordinates x and y at 3 different *ac* frequencies. As can be seen from Fig. 4B–G, $|Z|(x, y)$ and $\varphi(x, y)$ dependences are complex and drastically change with the frequency. Now the task is to estimate the following parameter sets: $R_s(x,y)$[4]; $R_{ct}(x,y)$; $C'_{DL}(x,y)$; $n(x,y)$; and $A_W(x,y)$ using the approach developed in this work (see Section 2).

The developed hybrid algorithm (as a part of the approach based on successive Bayesian estimation) demonstrated good stability of fitting in automatic mode; and the calculated values of the model parameters were exactly those same as used for the EIS data simulation. Fig. 5 shows the dependences of the main parameters $C'_{DL}(x,y)$; $n(x,y)$; $R_{ct}(x,y)$; and $A_W(x,y)$ of the model calculated from the dataset which is described in the beginning of the section and additionally illustrated in Fig. 4. The estimated errors of the parameter values were less than 0.0001%. The computational time to process the simulated dataset was 12 min 20 s using a 3 GHz processor (4GB RAM). The computation was performed in a background mode so that the user could use the desktop computer for other tasks in parallel.

This data proves the ability of the developed approach and the hybrid algorithm to accurately extract parameters of the model from multidimensional EIS datasets. This approach can likely be extended to real systems to process experimental data acquired by scanning electrochemical impedance spectroscopy.

4.2. Real-world dataset

To evaluate the performance of the developed approach and the hybrid algorithm in processing real-world experimental data, 720 electrochemical impedance spectra were recorded during the electrochemically driven intercalation of copper into tellurium from a 1 mM Cu^{2+} + 0.1 M $HClO_4$ aqueous electrolyte (see [42] for experimental details). These experimental impedance spectra were acquired as a function of the electrode potential and time to form a "5D" dependence (real part of impedance, imaginary part of impedance, probing *ac* frequency, electrode potential E, and intercalation time). 50 *ac* probing frequencies were used to record the spectra. The examples of the dependences of the modulus of impedance and the phase shift on the electrode potential and time at 2 different *ac* frequencies are shown in Fig. 6. The elucidated equivalent electric circuit (the physical model of the system) is shown in the inset of Fig. 1B.

The developed analysis method and the hybrid algorithm showed excellent performance and stability to process this large experimental dataset. It was possible to extract dependences of important parameters which characterise the electrode|electrolyte interface (e.g. the electric double layer capacitance and the apparent reaction rate coefficient of Cu^{2+} reduction) as a function of both time and the electrode potential. The latter dependences are shown in Fig. 7 as contour maps. In addition, the following individual parameter errors were estimated: (i) fluctuating in the range between 0.7% and 1.9% for $R_s(x,y)$; (ii) between 1.2% and 4.1% for $R_{ct}(x,y)$; between 4.5% and 20.5% for $A_W(x,y)$; between 0.9% and 2.4% for $C'_{DL}(x,y)$; and between 0.16% and 0.44% for $n(x,y)$. Relatively low estimated parameter errors confirm the significance of all the parameters of the model (1) to describe the impedance response.

The dependences presented in Fig. 7 show how the electrode|electrolyte interface dynamics change with both electrode potential and deposition time. Fig. 7A and B shows the dependences of the parameters which describe the electric double layer formed at the electrode|electrolyte interface. It reflects complex phenomena and molecule/ion rearrangements at the interface during intercalation (see ref. [42] for further electrochemical details for this system). The latter is particularly difficult

[2] The individual spectrum is the dependence of the real part of impedance and the imaginary part on the *ac* probing signal frequency, such as shown in Fig. 1A.

[3] Note that $Re[Z] = |Z| \cos\varphi$ and $Im[Z] = |Z| \sin\varphi$

[4] Constant values of $R_s(x,y)$ were used for simulations, as this parameter remains almost constant in real electrochemical experiments.

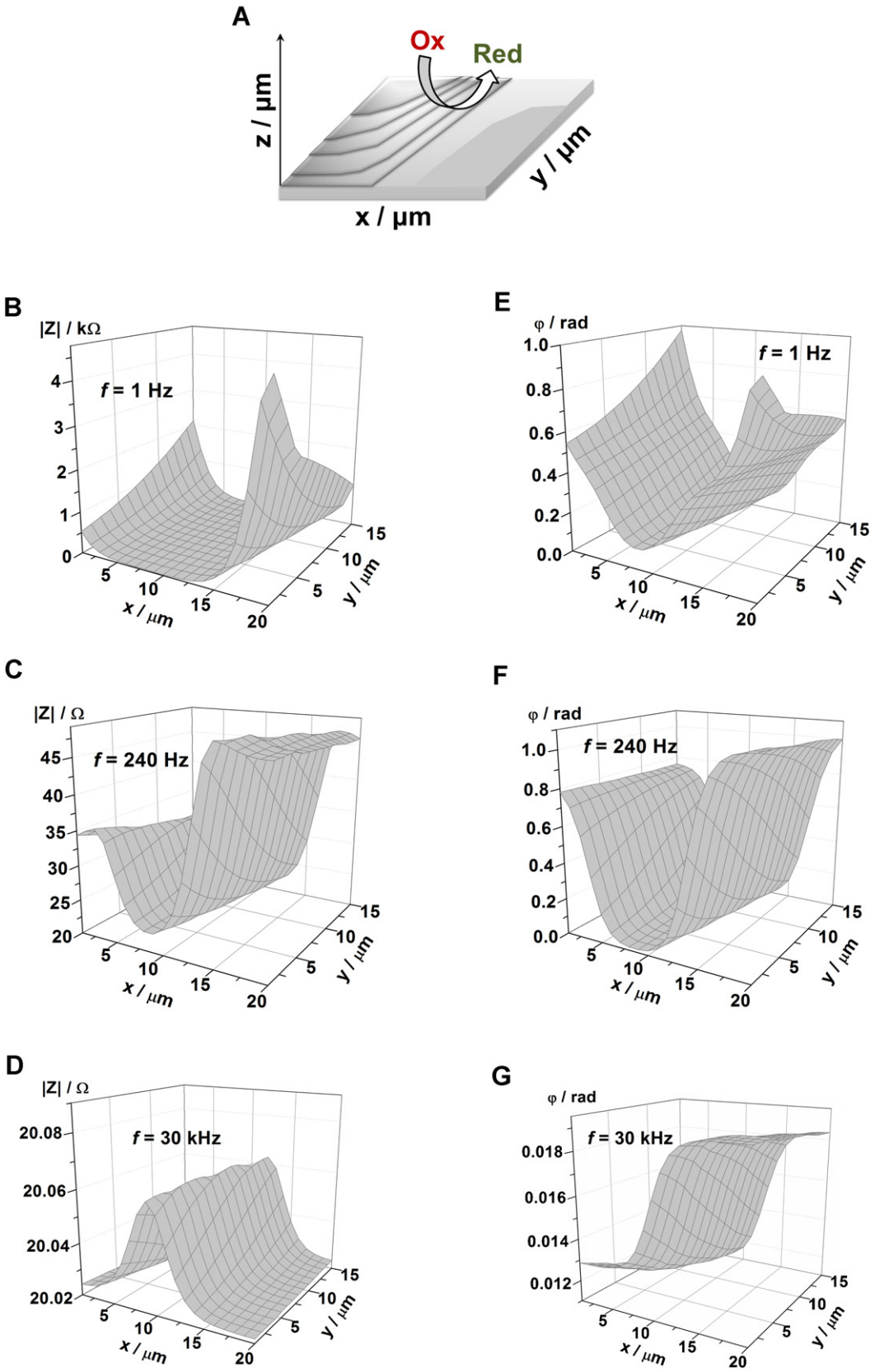

Fig. 4. (A) A hypothetical electrode surface and (B–G) simulated dependences of modulus of impedance, $|Z|$, and the phase shift, φ, on spatial coordinates x and y at 3 different *ac* frequencies, as indicated in the figure.

to monitor using conventional techniques and data processing approaches.

A pronounced minimum in Fig. 7C demonstrates that Cu^{2+} reduction at the surface is slow in the region which corresponds to electrode potentials between −0.33 V and −0.34 V and corresponding deposition time between 10 min and 23 min. This is likely due to the fact that the electrode surface is covered with Cu ad-atoms. It should be noted that deposition of more than one atomic layer of Cu is not possible at the Te surface at these potentials. Therefore, Fig. 7C shows where the transition from one rate determining step of intercalation (namely Cu^{2+} electrochemical reduction at the available Te surface) to another step occur (i.e., bulk diffusion of Cu

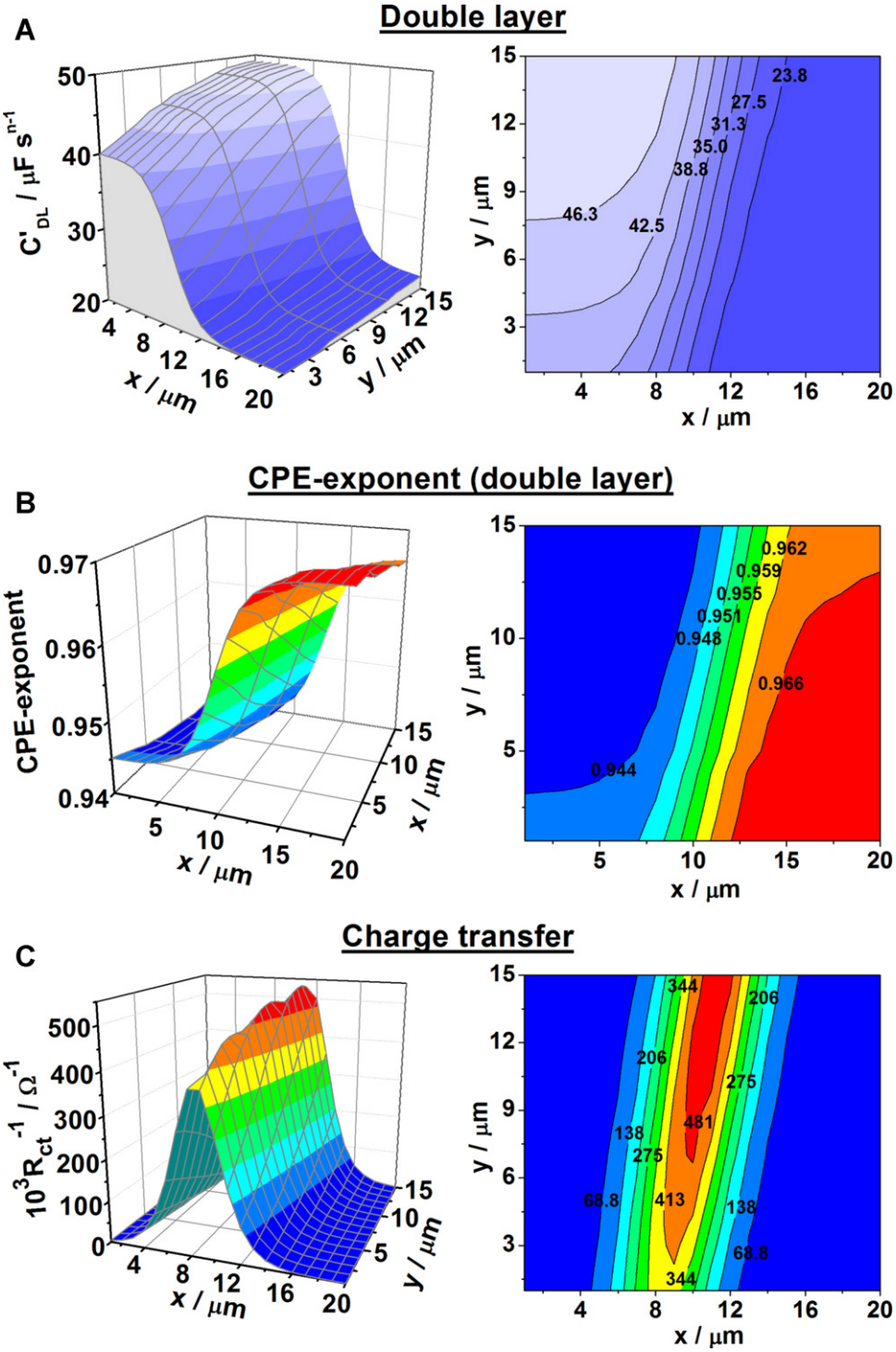

Fig. 5. (A, B) The parameters which describe the electric double layer: (A) C_{DL}, and (B) CPE-exponent, n, and (C, D) inverses of (C) the charge transfer resistance and (D) Warburg coefficient shown as a function of spatial coordinates x and y (300 data-points). The parameter values were extracted from simulated EIS data-sets using the approach developed in this work. The values found by the hybrid algorithm were exactly the same as used for the EIS data simulation.

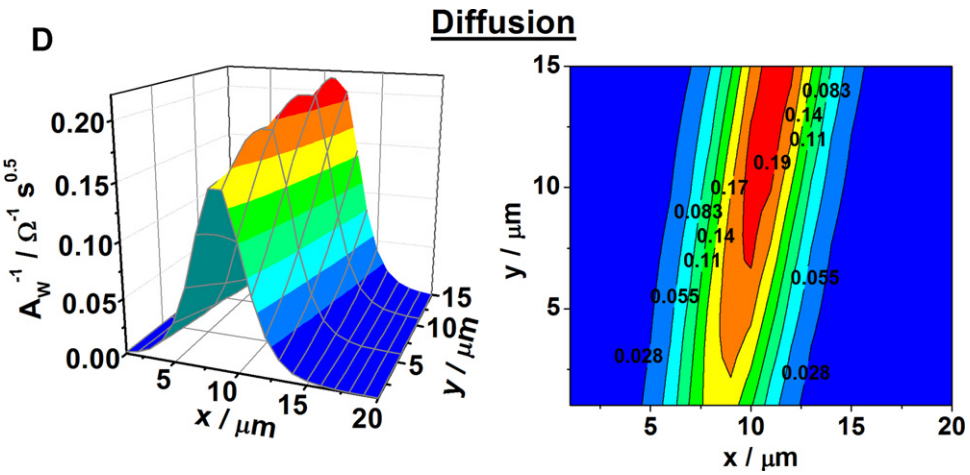

Fig. 5. (*Continued*)

which freeing the surface Te sites for further Cu electrochemical deposition). Additionally, Fig. 7D shows examples of "3D" EIS spectra (the parts with reduced dimensionality) together with fitting. The root-mean square deviations between experimental and fitted spectra were less than 2% in all cases.

It should be noted here that apart from the fact that the only one EIS-model has been considered in this work, the developed approach (and the hybrid algorithm as the part of the approach) has also shown promising performance in the analysis of experimental datasets where more complex models were used. These models described (i) deposition of atomic layers of metals in presence of specific adsorption of other electrolyte components [10], (ii) an electrocatalytic reaction (nitrate reduction) which occur simultaneously with formation of the catalyst layers [9], and (iii) where adsorption and desorption of different anions and cations occur simultaneously [43].

The examples shown above demonstrate the true potential of multidimensional data acquisition and analysis in EIS, if the

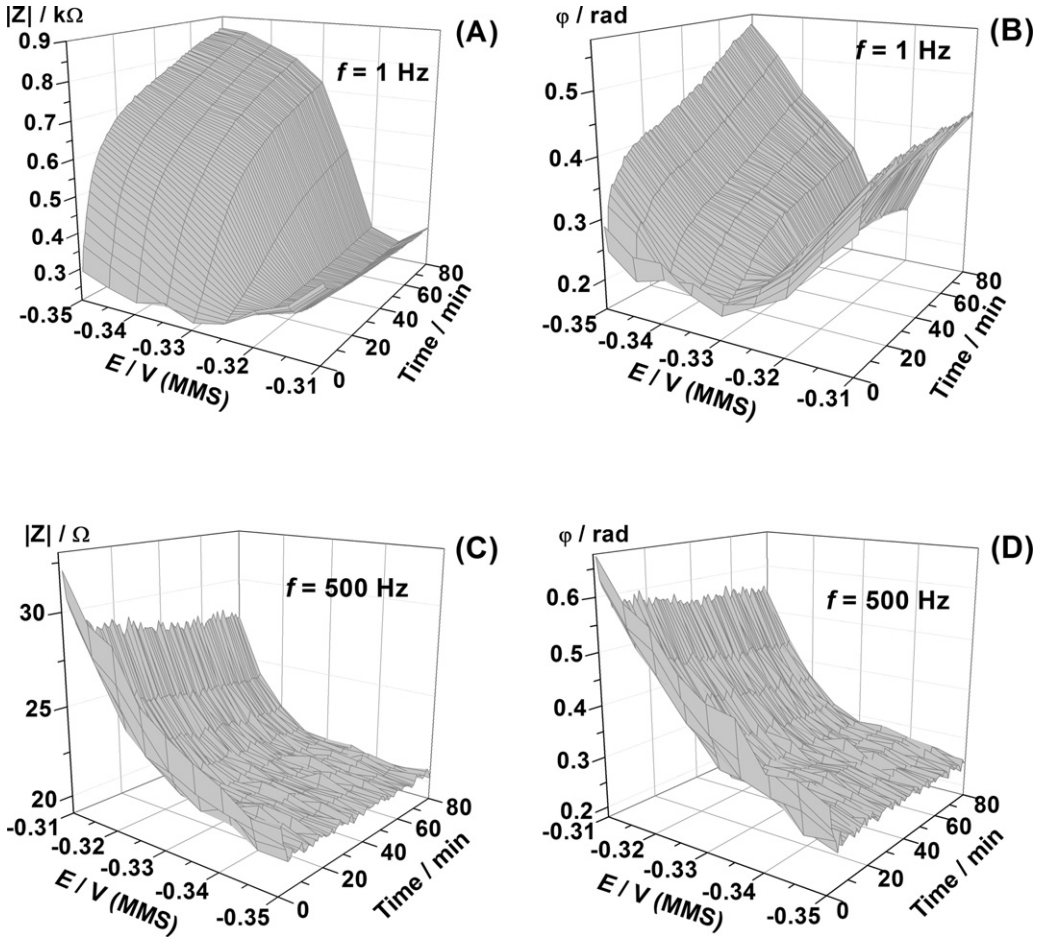

Fig. 6. Experimental EIS dataset: dependences of modulus of impedance, $|Z|$, and the phase shift, φ, on the electrode potential E and time shown at 2 different *ac* frequencies, as indicated in the figure.

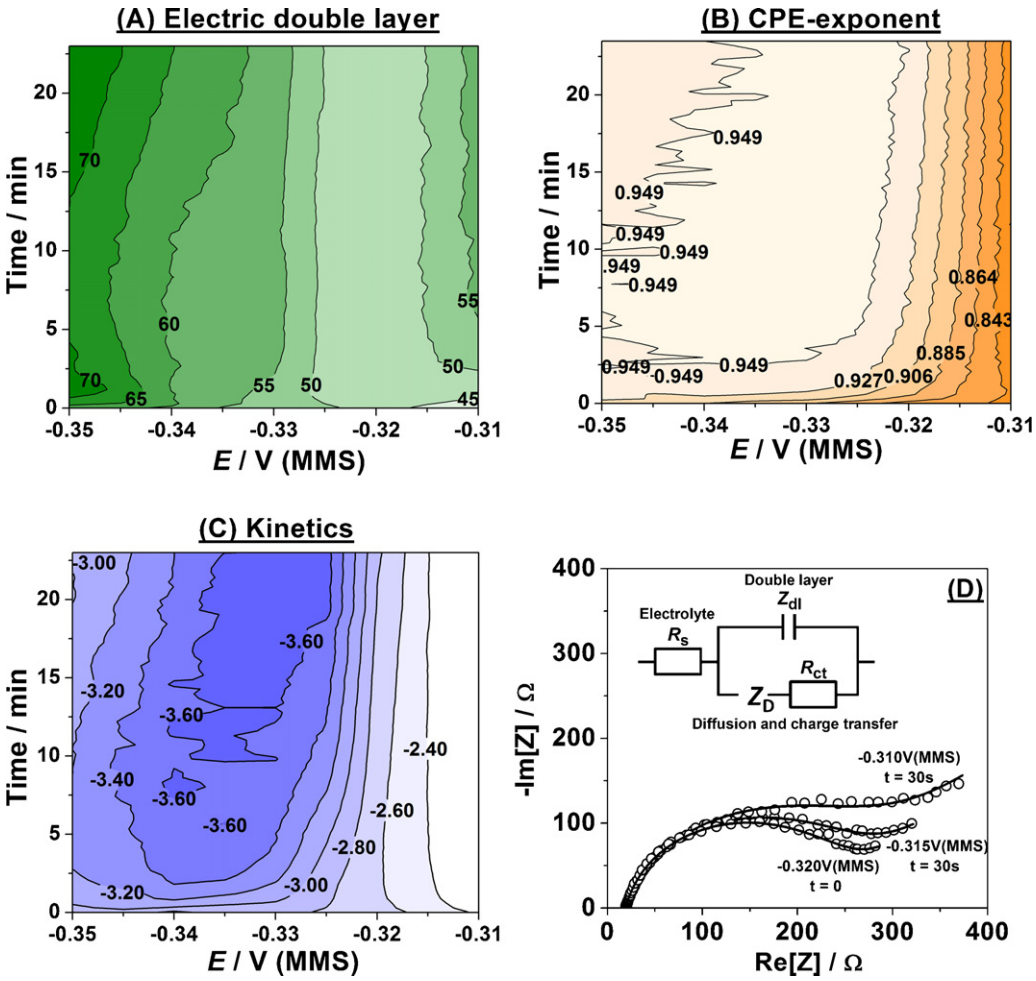

Fig. 7. Variations of (A) the electric double layer parameter C'_{DL} (this parameter is proportional to the electric double layer capacitance, C_{DL}, where the double layer impedance is given as $Z_{dl} = C'^{-1}_{DL}[j2\pi f]^{-n}$ (j is the imaginary unit and exponent n vary in the range $0.7 \le n \le 1$)), (B) CPE-exponent and (C) a surface kinetic parameter (in the *log* scale) calculated as $(2D)^{0.5}A_W R_{ct}^{-1}$, where D is the diffusion coefficient for Cu^{2+} [42], during electrochemically driven intercalation of copper into tellurium from a 1 mM Cu^{2+} + 0.1 M $HClO_4$ aqueous electrolyte. The parameter variations were obtained by processing experimental EIS data. The electrode potentials are given versus mercury/mercury sulphate (MMS) reference electrode. (D) Examples of spectra and fitting (solid lines) at some selected times and potentials.
Adapted from [42].

appropriate data analysis approaches and fitting algorithms are used. Successive Bayesian estimation combined with efficient minimisation algorithms to allow processing of large data-sets is a promising route to many further improvements in the field of impedance spectroscopy.

5. Conclusions

An approach for the analysis of large experimental datasets in EIS has been developed. The approach uses successive Bayesian estimation, splits the multidimensional impedance datasets into parts with reduced dimensionality. Estimation of the parameters of the models is performed successively, from one part to another, using CNLS method. In this successive procedure, the results obtained on the previous step are used as *a priori* values for the analysis of the next part. To provide high stability of the sequential CNLS minimisation procedure, a new hybrid algorithm has been developed. This algorithm uses a combination of a modified Powell and Nelder–Mead simplex (with constraints) minimisation strategies. The algorithm provides the required stability of the iterative procedures which allows semi-automatic processing of large impedance datasets.

The developed data optimisation strategy can be further extended to other EIS applications which require multidimensional data analysis. The algorithm does not require the calculation of derivatives, is easy to implement and modify for different specific applications.

Acknowledgments

I would like to thank Prof. Dr. Alexey L. Pomerantsev (Semenov Institute of Chemical Physics RAS, Moscow, Russia) for valuable suggestions about this manuscript.

I would also like to thank my colleagues: Dr. Minghua Huang (CES, Ruhr-Universität Bochum) for the experimental data-set acquisition and Dr. John B. Henry (CES, Ruhr-Universität Bochum) for proofreading. I am also thankful to Dr. Genady Ragoisha (Belarusian State University, Belarus) and Mr. Balazs B. Berkes (Eötvös Loránd University, Hungary) for valuable comments and remarks about the performance of the hybrid algorithm. The developed approach and the hybrid algorithm have also been independently tested by Dr. Benjamin Sanchez (Universitat Politecnica de Catalunya, Spain, November–December 2011) using bio-impedance data acquired *in vivo* and by Mr. Balazs B. Berkes (Eötvös Loránd University, Hungary, January–September

2011) using different electrochemical systems. The work was supported in part by the EU and the state NRW in the framework of the HighTech.NRW program.

References

[1] M.E. Orazem, B. Tribollet, Electrochemical Impedance Spectroscopy, John Wiley and Sons, Hoboken, 2008, 523 pp.
[2] B.Y. Chang, S.M. Park, Annu. Rev. Anal. Chem. 3 (2010) 207.
[3] A.J. Bard, L.R. Faulkner (Eds.), Electrochemical Methods: Fundamentals and Applications, 2nd ed., Wiley, New York, 2001 (Chapter 17).
[4] M.L. Moraesa, L. Petri, V. Oliveira, C.A. Olivati, M.C.F. de Oliveira, F.V. Paulovich, O.N. Oliveira Jr., M. Ferreira, Sens. Actuator B 166–167 (2012) 231–238.
[5] M.L. Moraes, R.M. Maki, F.V. Paulovich, U.P. Rodrigues Filho, M.C.F. de Oliveira, A. Riul, N.C. de Souza Jr., M. Ferreira, H.L. Gomes, O.N. Oliveira Jr., Anal. Chem. 82 (2010) 3239–3246.
[6] F.V. Paulovich, M.L. Moraes, R.M. Maki, M. Ferreira, O.N. Oliveira Jr., M.C.F. de Oliveira, Analyst 136 (2011) 1344–1350.
[7] C.M. Pettit, P.C. Goonetilleke, C.M. Sulyma, D. Roy, Anal. Chem. 78 (2006) 3723.
[8] O.L. Blajiev, T. Breugelmans, R. Pintelon, H. Terryn, A. Hubin, Electrochim. Acta 53 (2008) 7451.
[9] M. Huang, J.B. Henry, B.B. Berkes, A. Maljusch, W. Schuhmann, A.S. Bondarenko, Analyst 137 (2012) 631.
[10] B.B. Berkes, A. Maljusch, W. Schuhmann, A.S. Bondarenko, J. Phys. Chem. C 115 (2011) 9122.
[11] B. Sanchez, G. Vandersteen, R. Bragos, J. Schoukens, Meas. Sci. Technol. 22 (2011) 115601.
[12] E.V. Bystritskaya, A.L. Pomerantsev, O.Ye. Rodionova, J. Chemometr. 14 (2000) 667.
[13] A.L. Pomerantsev, Chemometr. Intell. Lab. 66 (2003) 127–139.
[14] O.E. Rodionova, A.L. Pomerantsev, Kinet. Catal. 45 (2004) 455.
[15] E. Barsoukov, J.R. Macdonald, Impedance Spectroscopy: Theory, Experiment, and Applications, Wiley, New Jersey, 2005, pp. 195–197.
[16] A. Lasia, in: B.E. Conway, J. Bockris, R.E. White (Eds.), Modern Aspects of Electrochemistry, vol. 32, Kluwer Academic/Plenum Publishers, New York, 1999, pp. 143–248.
[17] J.R. Macdonald, J.A. Garber, J. Electrochem. Soc. 124 (7) (1977) 1022.
[18] B.A. Boukamp, Solid State Ionics 20 (1986) 31.
[19] B.A. Boukamp, Solid State Ionics 18–19 (1986) 136.
[20] J.R. Macdonald, L.D. Potter Jr., Solid State Ionics 24 (1) (1987) 61.
[21] J.R. Macdonald, Solid State Ionics 58 (1–2) (1992) 97.
[22] ZSimpWin, Version 3.30, http://www.echemsw.com/prod01.htm, 2012.
[23] D. Marquardt, SIAM J. Appl. Math. 11 (1963) 431.
[24] W.H. Press, S.A. Teukolsky, W.T. Vetterling, B.P. Flannery, Numerical Recipes in C++, 2002 (Chapter 15:5).
[25] J.A. Nelder, R. Mead, Comput. J. 7 (1964) 308.
[26] T.J. VanderNoot, I. Abrahams, J. Electroanal. Chem. 448 (1998) 17.
[27] D. Vladikova, Z. Stoynov, J. Electroanal. Chem. 572 (2004) 377–387.
[28] A.S. Bondarenko, G.A. Ragoisha, in: A.L. Pomerantsev (Ed.), Progress in Chemometrics Research, Nova Science Publishers, New York, 2005, pp. 89–102.
[29] G.A. Ragoisha, N.P. Osipovich, A.S. Bondarenko, J. Zhang, S. Kocha, A. Iiyama, J. Solid State Electrochem. 14 (2010) 531–542.
[30] A.S. Bondarenko, I.E.L. Stephens, H.A. Hansen, F.J. Perez-Alonso, V. Tripkovic, T.P. Johansson, J. Rossmeisl, J.K. Nørskov, I. Chorkendorff, Langmuir 27 (2011) 2058–2066.
[31] A.S. Bondarenko, G.A. Ragoisha, N.P. Osipovich, E.A. Streltsov, Electrochem. Commun. 8 (2006) 921–926.
[32] G.A. Ragoisha, A.S. Bondarenko, Surf. Sci. 566–568 (2004) 315–320.
[33] G.A. Ragoisha, A.S. Bondarenko, N.P. Osipovich, E.A. Streltsov, Electrochim. Acta 53 (2008) 3879–3888.
[34] G.A. Ragoisha, A.S. Bondarenko, Solid State Phenom. 90–91 (2003) 103–108.
[35] G.B. Dantzig, Origins of the simplex method, in: S.G. Nash (Ed.), A History of Scientific Computing, Reading, ACM, NY, USA, 1990, pp. 141–151.
[36] C.G. Broyden, J. Inst. Maths. Appl. 6 (1970) 76.
[37] R. Fletcher, Comput. J. 13 (1970) 317.
[38] D. Goldfarb, Math. Comp. 24 (1970) 23.
[39] D.F. Shanno, Math. Comp. 24 (1970) 647.
[40] K. Eckhard, W. Schuhmann, Analyst 133 (2008) 1486.
[41] K. Eckhard, T. Erichsen, M. Stratmann, W. Schuhmann, Chem. Eur. J. 14 (2008) 3968.
[42] M. Huang, A. Maljusch, J.B. Henry, W. Schuhmann, A.S. Bondarenko, Electrochem. Commun. 20 (2012) 92–96.
[43] B.B. Berkes, G. Inzelt, W. Schuhmann, A.S. Bondarenko, J. Phys. Chem. C 116 (2012) 10995–11003.